Available online at www.sciencedirect.com
SCIENCE DIRECT®
European Journal of Medicinal Chemistry 39 (2004) 959–967
EUROPEAN JOURNAL OF MEDICINAL CHEMISTRY
www.elsevier.com/locate/ejmech

Original article

# Homology modelling and binding site mapping of the human histamine H1 receptor

Róbert Kiss [a], Zoltán Kovári [a,b], György M. Keserű [a,b,*]

[a] *Department of Computer Assisted Drug Discovery, Gedeon Richter Ltd., H-1475, Budapest 10, P.O. Box 27, Hungary*
[b] *Department of Chemical Information Technologies, Budapest University of Technology and Economics, H-1111, Budapest, Szt. Gellért tér 4, Hungary*

Received 4 March 2004; received in revised form 26 July 2004; accepted 30 July 2004

Available online 15 September 2004

**Abstract**

Three-dimensional model of the human histamine H1 receptor was developed by homology modelling using the high resolution structure of bovine rhodopsin as template. Genetic algorithm based docking calculations were used to identify the role of several amino acids having an effect on agonist or antagonist binding. Binding mode analyses of mepyramine, desloratidine, loratidine and acrivastine allowed us to rationalise their binding affinity. Binding site mapping resulted in seven new potential aromatic interaction points (Tyr 108, Phe 184, Phe 190, Phe 199, Phe 424, Trp 428, Tyr 431), that took part in forming the lipophilic pocket of the antagonist binding cavity.


*Keywords:* Human histamine H1 receptor; Homology model; Binding site mapping; Antagonist

## 1. Introduction

Histamine is one of the most frequently studied local hormones, which plays a major role in several physiological processes. Up to now, four of its target proteins have been cloned (H1, H2, H3, and H4 receptors) from among which H1 and H2 receptors are assigned to have an overriding pharmaceutical importance. The H1 receptor is mainly responsible for the inflammatory effect of histamine, e.g. smooth muscle contraction, increasing blood vessel permeability, releasing other local hormones [1]. Therefore, it is the target of most drugs developed against allergic rhinitis. By means of the H2 receptors histamine is responsible for the stomach's hydrochloric acid production, which makes it possible to treat ulcer with H2 antagonists. Several effective and selective H2 antagonists are available, that can be used without any serious side effect [1]. The H3 receptor can enhance some neurotransmitter's release. A few H3 antagonists have already been developed for the treatment of neurological and cognitive disorders, but the efficiency of these compounds have not been confirmed reassuringly yet [2]. The H4 receptor was cloned just a few years ago [3], and there is not sufficient information about its physiological effects, but it seems to play a role in histaminergic receptor mediated chemotaxis [4].

Up to now, developing new antihistamine compounds were almost exclusively based on modifying the structure of some accidentally discovered H1 antagonists (e.g. mepyramine) and histamine itself. Cloning HHR1, however, opened new ways to examine the binding of histamine and its antagonists, and to find the important receptor–ligand interaction points. Comparative sequence analyses followed by site-directed mutagenesis studies revealed the importance of particular residues at the binding site of the receptor. However, data from site-directed mutagenesis studies have got to be evaluated with caution, especially in the case of G-protein coupled receptors (GPCR). HHR1 is a GPCR containing seven transmembrane (TM) α-helices. These TM regions comprise conserved residues, that are of importance in forming the helical structure and in signalling [5]. For example, some tryptophan residues in well-defined positions of GPCRs are responsible for forming the required alpha-helical secondary structural elements in the TM domain. Mutating these tryptophans inactivates the receptor, since the mutations alter the contacts to the phospholipid bilayer [6]. Loosing affinity therefore could also mean, that the mutated

*Abbreviations:* HHR1, human histamine H1 receptor; GPCR, G-protein coupled receptor; TM, transmembrane domain; BBB, blood brain barrier; EC, extracellular; IC, intracellular.

* Corresponding author. Tel.: +36-1-4314605; fax: +36-1-4326002.
*E-mail address:* gy.keseru@richter.hu (G.M. Keserű).

0223-5234/$ - see front matter © 2004 Elsevier SAS. All rights reserved.
doi:10.1016/j.ejmech.2004.07.009

residue is essential for the formation of the receptor's helical structure, not necessarily in the binding site formation.

First-generation H1 antagonist compounds (mepyramine, chlorpheniramine, diphenhydramine, piperoxan, etc) were proved to be effective through their strong histamine-inhibiting ability, however, they cause sedation. This side effect is suspected to attain due muscarinic receptors or H1 receptors in the central nervous system [1,7]. Second-generation H1 antagonists (acrivastine, loratadine, cetirizine, terfenadine, etc) are significantly less sedative, because of higher selectivity and the reduced level of crossing the blood brain barrier (BBB). Nevertheless, the most selective second-generation antagonists, widely used in clinical practice, have much lower affinity for H1 receptor, than the first-generation mepyramine. Cetirizine seems to be one of the most selective ligands for HHR1 [8], but its affinity is 30 times lower, than mepyramine's. Similarly, loratadine is 80 times less potent, than mepyramine [9]. Loratadine and cetirizine are the active ingredients of the most frequently used antihistamine drugs today. Other potent H1 antagonists (astemizole, terfenadine) can cause cardiovascular side effects [10,11]. Recently, a new generation of antihistamines seems to appear, since desloratadine and olopatadine—two highly effective, and non-sedating H1 antagonist compounds—were made over. No serious side effects of these compounds have been reported yet.

HHR1 ligands have typically a protonated amine function, which interacts with the conserved side chain of Asp 107 in TM3. This was proved by the D107A mutation [12], resulting in loss of affinity of both the agonist and antagonist binding. The only ligand that showed an intermediate binding to this mutant receptor was olopatadine [8]. This conserved aspartate can be found in virtually all monoamine receptors. Further site-directed mutagenesis studies showed, that the N($\tau$)-H part of the imidazole ring of histamine interacts with Asn 198 [12]. Mutagenesis studies on guinea pig histamine H1 receptor have revealed, that Lys 200 (Lys 191 in HHR1) and Trp 167 (Trp 158 in HHR1) are important interaction points for histamine [6,13]. Three residues were mutated in guinea pig H1 receptors to determine the lipophilic site of the antagonist binding pocket [6]. Phe 433 (Phe 432 in HHR1) seemed to be essential, Phe 436 (Phe 435 in HHR1) and Trp 167 (Trp 158 in HHR1) were also very important for efficient antagonist binding.

Mepyramine is a typical member of the first-generation H1 antagonists. It has high affinity and selectivity for HHR1, but causes sedation due to crossing the BBB and binding to H1 receptors of the central nervous system. There is a large number of first-generation H1 antagonists, that differ just in smaller modifications from the mepyramine-structure (chlorpheniramine, diphenhydramine, tripelennamine, triprolidine, chlorcyclizine, chloropyramine) (Fig. 1). These molecules contain two aryl groups with additional small electron-donating substituents in para-position. The protonated amine function is at a distance of 3–4 bonds from the aromatic rings.

Some phenothiazine-derivates, such as promethazine and chlorpromazine in therapeutical use were observed to ease

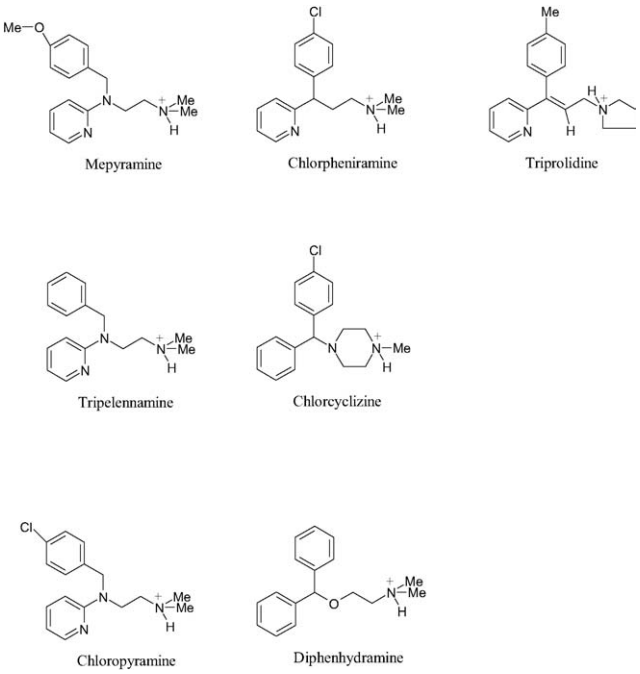


Fig. 1. Mepyramine and structurally analogous H1 antagonists.

the symptoms of allergy, therefore development of H1 antagonists has headed towards a new way (Fig. 2).

The tricyclic dibenzoazepine structure seemed to be a promising starting point for designing new potent antihistamines. Doxepin, epinastine and ketotifen have high affinity for HHR1, but also for other receptors [8]. More selective ligands with a tricyclic structure were synthesized of which desloratadine [14], loratadine [15] and olopatadine [8] were found to be potent and selective.

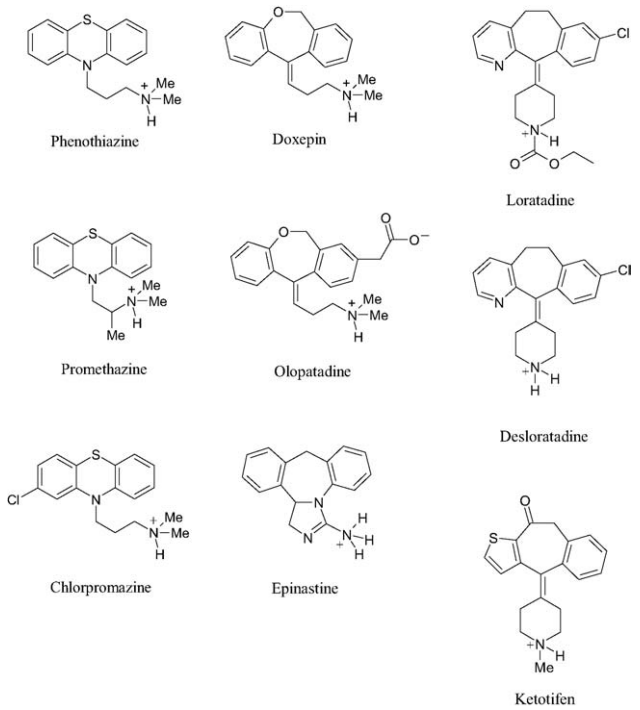


Fig. 2. Tricyclic H1 antagonists.

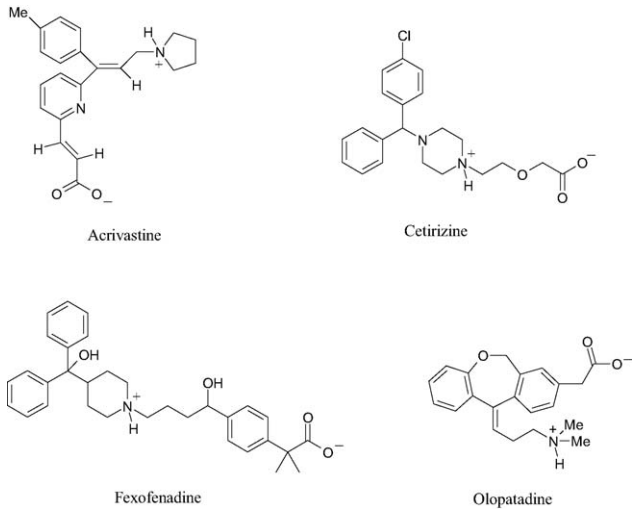


Fig. 3. Zwitterionic H1 antagonists.

On the other hand zwitterionic ligands (acrivastine, cetirizine, olopatadine, fexofenadine) show high selectivity, that suggests a specific interaction between their carboxylate residue and a protonated amino acid in HHR1 (Fig. 3) [6]. This second ionic interaction possibly provides the conditions for designing new potent, selective H1 antagonists, that do not cross the BBB.

HHR1 is a typical 7TM GPCR consisting of two soluble domains and seven transmembrane helices. Availability of the high resolution structure of bovine rhodopsin as well as the large number of mutational data prompted us to build a homology model of HHR1. Several useful information have already been published by means of GPCR homology models [16,17], and eligibility of these models for docking procedures has also been proven [18]. Accordingly, we selected four known H1 antagonists for docking into our receptor model. We chose mepyramine from the first-generation diaryl-antihistamines, desloratadine and loratadine from the second-generation tricyclic antihistamines, and the second-generation acrivastine containing a carboxylate residue. These molecules embrace almost every binding possibilities of the H1 antagonists, apart from a few special structure. Published mutation data were used to identify the antagonist binding site and validating the homology model.

Based on the flexible docking of typical H1 antagonists to our homology model we were able to explore the architecture of their binding site as well as their interactions with HHR1. Binding affinities of these compounds were rationalized and our binding site mapping revealed an additional hydrophobic cavity to be targeted by new H1 antagonists.

## 2. Experimental protocols

### 2.1. Sequence alignment

Comparative sequence analysis between HHR1 and bovine rhodopsin was performed by Clustal W [19]. GPCRs' TM domain show higher homology, than the extracellular (EC) or intracellular (IC) domains. The long IC3 loop of HHR1 was excluded from modelling, since it has no equivalent in the bovine rhodopsin sequence. Here, we have to mention that the bovine rhodopsin crystal structure is in its inactive conformation, therefore we assumed that homology modelling of the antagonist binding site is reasonable.

The sequence alignment (without IC3 of HHR1) resulted in the following homology data: 15.20% of the residues are identical, 25.73% strongly similar, 10.82% weakly similar and 48.25% different.

The bovine rhodopsin structure contains a disulfide-bond between residues Cys 110 and Cys 187. In the sequence alignment two cysteins of HHR1 got into the same positions, therefore we assumed that Cys 100 and Cys 180 form a disulfide-bond in the HHR1. The automatic sequence alignment was followed by manual adjustment, paying attention to the position of the conserved GPCR residues.

### 2.2. Homology modelling and validation

Six HHR1 initial models were built by MODELLER version 4 [20], using the above described sequence alignment and the bovine rhodopsin crystal structure (PDB ID: 1F88) [21]. Modeller was run with default parameters, with the option of disulfide bridge assignment. The main geometric parameters of the models were determined by PROCHECK [22]. We chose the first model for further investigations, which possesses on average the most favourable features.

In the last step of homology modelling the selected model was subjected to a series of tests for its internal consistency and reliability. Backbone conformation was evaluated by the inspection of the Psi/Phi Ramachandran plot obtained from PROCHECK analysis. The PROSA [23] test was applied to check for energy criteria in comparison with the potential of mean force derived from a large set of known protein structures. Packing quality of the homology model was investigated by the calculation of WHATIF Quality Control value [24].

### 2.3. Binding mode analysis

The homology model of HHR1 was used for docking antagonists into the binding site suggested by site-directed mutagenesis studies. All of the antagonists were first subjected to p$K_a$ evaluation to consider their protonation state at physiological pH. p$K_a$ values of histamine, mepyramine, desloratadine and loratadine were retrieved from references (10.13 [25], 6.43 [25]; 8.92 [26]; 8.65 [26]; 4.58 [26], respectively). p$K_a$ values of acrivastine (2.82, 7.59) were calculated by CompuDrug's Pallas software [27].

Before starting the docking procedure we represented the channel surfaces of our receptor model, using the Multi Channel Surfaces module as implemented in Sybyl 6.9 [28] with a 1.4 Å probe radius. A considerable cavity was found in the TM region of the receptor, in close proximity to the

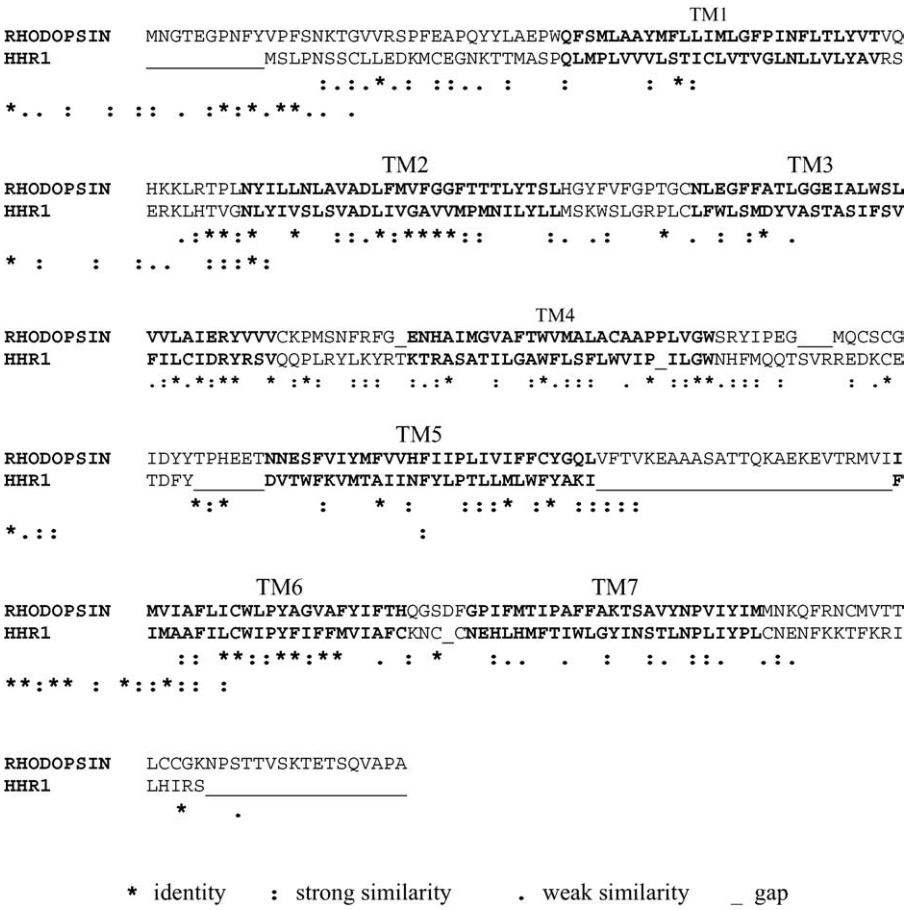


Fig. 4. Alignment of the amino acid sequences of bovine rhodopsin and HHR1 (without IC3 of HHR1).

conserved Asp 107 which was supposed to be one of the most crucial residues of the ligand binding in HHR1.

All docking calculations were performed by the genetic algorithm based flexible docking code, FlexiDock as implemented in Sybyl 6.9. Running FlexiDock with default parameters resulted in insufficient docking solutions. Since we concluded that the lack of reliable solutions could be caused by the insufficient sampling efficacy, parameters of the island genetic algorithm [29] were changed. The number of islands was set from 1 to 50 that resulted in an increased number of multiple, independent populations that were maintained during the docking run. The maximum number of members saved per island was set from 20 to 50 and consequently we increased the number of members that were redistributed among other islands. The population size for all islands was set from 500 to 1500 and the full mutation chance per gene was increased from 0.1 to 0.3. These changes contributed to higher diversity of sampled configuration of genes and allowed us to achieve sufficient sampling of the conformational space available for ligands within the binding site.

## 3. Results

### *3.1. Homology modelling*

The final alignment of the HHR1 sequence to that of bovine rhodopsin is shown in Fig. 4. Besides the insertions and deletions detected in loop regions corresponding to TM regions of bovine rhodopsin there is only a single gap detected in TM4. It should be noted, however, that this gap is located at the AAPPLV motif of bovine rhodopsin (VIP_IL in HHR1) where prolines disrupted the helicity of TM4. Considering only the TM regions, percentages of homologous residues in TM1–TM7 are 63%, 63%, 65%, 65%, 68%, 65%, and 64%, respectively.

Our alignment was carefully checked in TM regions and we found that all of the critical structural elements involved in the binding of its natural substrate, histamine are intact. Therefore, we conclude that this alignment can be used to construct a reliable 3D model for HHR1 binding site.

The results of PROCHECK analysis obtained for the six models are collected in Table 1. Given the relatively low percentage of residues having Phi/Psi angles in the disallowed ranges, the quality of Ramachandran plots is acceptable for all models. Goodness factors calculated both for covalent and non-covalent interactions suggest models 1, 2 and 5 to be superior than that of the other models. Analysis of bad contacts, bond lengths, bond angles, and improper torsions revealed model 1 to be an optimal choice. Molecular PDF values obtained by MODELLER also suggested this model for further studies.

Validation of the homology model involved three independent tests. The first test was to compare the residue backbone

Table 1
Main geometric parameters of the six HHR1 models developed by MODELLER

| HHR1 models | Ramachandran plot | | | | Bad contacts | G-factor | M/c bond lengths (%) | M/c bond angles (%) | Planar groups (%) |
|---|---|---|---|---|---|---|---|---|---|
| | Core (%) | Allow (%) | Gener (%) | Disall (%) | | | | | |
| 1 | 83.0 | 15.4 | 0.8 | 0.8 | 9 | –0.15 | 90.2 | 73.9 | 100 |
| 2 | 79.5 | 19.3 | 0.8 | 0.4 | 12 | –0.14 | 88.6 | 74.9 | 96.0 |
| 3 | 81.1 | 15.4 | 3.5 | 0 | 12 | –0.22 | 84.5 | 70.0 | 100 |
| *4* | 81.1 | 16.2 | 2.3 | 0.4 | 11 | –0.20 | 89.9 | 74.6 | 94.4 |
| 5 | 84.2 | 13.9 | 0.8 | 1.2 | 7 | –0.16 | 89.6 | 71.7 | 96.7 |
| 6 | 81.1 | 15.1 | 3.5 | 0.4 | 12 | –0.18 | 91.0 | 72.6 | 100 |

conformations in our model with the preferred values obtained from the Protein Data Bank of known structures. As shown in the Ramachandran plot of Fig. 5, the distribution of the Phi/Psi angles of the model is within the allowed regions. Only two out of the 282 (0.8%) residues have disallowed conformations. Comparing this result with that obtained for the bovine rhodopsin served as our template we found one residue located in disallowed regions. Thus, our analysis suggests the backbone conformations of our HHR1 model to be nearly as good as those of the template.

The second test of the HHR1 model was to apply energy criteria using PROSA. We investigated whether the interaction energy of each residue with the remainder of the protein is negative. PROSA energy plots for the HHR1 model and bovine rhodopsin are shown in Fig. 6. It can be seen that the overall graph is quite similar for both the experimental bovine rhodopsin structure and the HHR1 model having negative or low positive interaction energies. On the other hand, however, residues 170–180 of HHR1 have the most positive PROSA energies indicating unfavourable interactions in this region. Since this part of the sequence belongs to EC3 which does not participate in neither ligand binding nor receptor activation we concluded that our HHR1 model performs pretty much the same in the PROSA test as the template.

The third test used to evaluate our HHR1 model was to compare the packing environment for residues of the same type in high quality experimental structures deposited in the Protein Data Bank using the WHATIF program. A residue in a model structure with a score of –5.0 or worse usually indicates poor packing. Fig. 7 shows the scores for HHR1 model and for the template, as well. Since there have been even less residues with a score of –5.0 or lower in our HHR1 model than that in our template (5 and 9 residues, respectively) we concluded that the model represents an acceptable

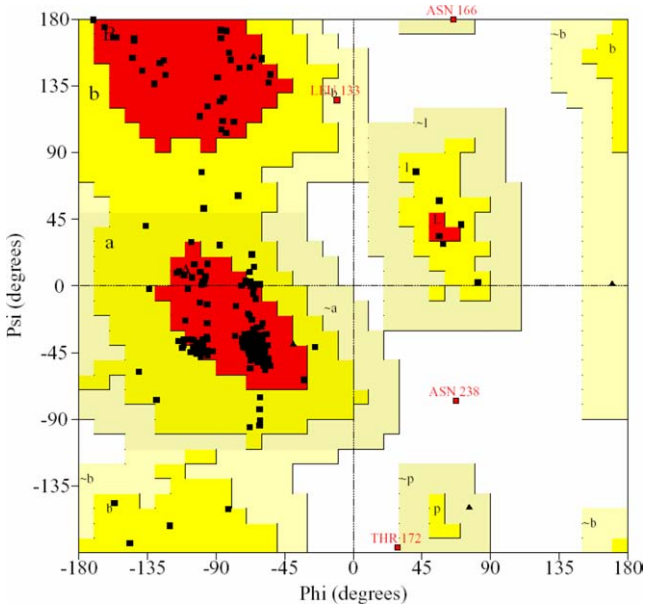


Fig. 5. Ramachandran plot of the HHR1 model. The most favoured regions are coloured red, additional allowed, generously allowed and disallowed regions are indicated as yellow, light yellow and white fields, respectively.

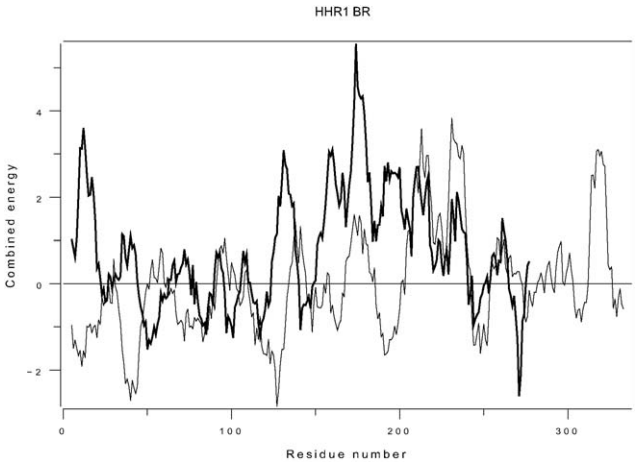


Fig. 6. PROSA plot calculated for HHR1 model (bold line) and for the template (normal line).

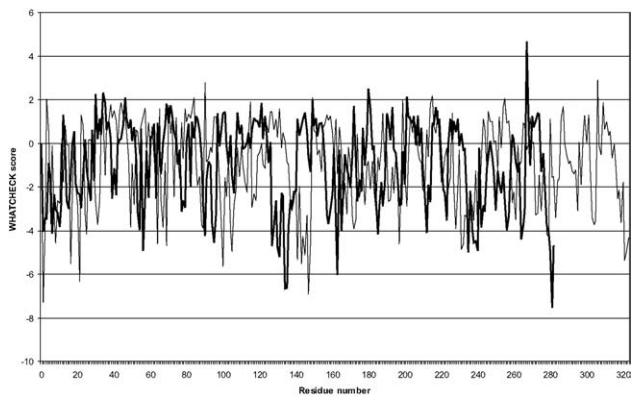


Fig. 7. WHATIF coarse packing values calculated for HHR1 model (bold line) and for the template (normal line).

packing quality when compared to the only available GPCR X-ray structure.

In summary, the quality of our HHR1 model has been checked using three different types of criteria. The results showed that the backbone conformation (PROCHECK), the residue interaction (PROSA) and the residue contact (WHATIF) are well within the limits established for reliable structures. Passing all tests by our structure suggests that we obtained an adequate model for HHR1 to characterize its binding site and to explore interactions formed with different antagonists.

### 3.2. Architecture of the agonist binding site

To see how an agonist can anchor at the HHR1, we tried to dock histamine into the binding cavity assigned by the compounds that affect in histamine binding, according to mutation data. Side chains of these amino acids (Asp 107 in TM3, Trp 158 in TM4, Asn 198 and Lys 191 in TM5) were orientated in a favourable position, since the binding cavity let these side chains move freely. After these modifications we found, that histamine is in a favourable position to reach Asp 107 and Asn 198, the imidazole-ring can create a lipophilic interaction with Trp 158, however Lys 191 is any farther than a strong H-bond would need with histamine. However, one has to keep in mind that the HHR1 model was based on the inactive conformation of bovine rhodopsin, therefore agonist binding cannot be properly modelled.

### 3.3. Architecture of the antagonist binding site

Residues, that were proved to take part in antagonist binding (Trp 158, Phe 432, Phe 435) [6], were in favourable positions to form a lipophilic cavity. Trp 165 and Phe 434 were found to be oriented to the phospholipid membrane, in keeping with W174A (W165A in HHR1) and F435A (F434A in HHR1) mutation analysis data on guinea pig receptor—these mutant receptors did not show remarkably different antagonist binding from the wild-type guinea pig H1 receptor [6]. Another tryptophan residue in TM4 (Trp 152) was far away from the binding pocket, however, according to mutation data this residue is an essential part of HHR1 [6]. We found other aromatic residues, that are potential lipophilic interaction points in TM3 (Tyr 108), at the end of EC3 (Phe 184), in TM5 (Phe 190, Phe 199) and in TM6 (Phe 424, Trp 428, Tyr 431). These were used as parts of the binding pocket in the docking process. Lys 191 in TM5 was found in the internal side of the receptor, and seemed to be able to create an ionic interaction with the carboxylate group of zwitterionic H1 antagonists.

### 3.4. Binding mode analysis for H1 antagonists

Docking simulations of the four H1 antagonist molecules (i.e. mepyramine, desloratidine, loratidine, and acrivastine) were performed by FlexiDock docking software as implemented in Sybyl 6.9 [28]. Our homology model's backbone structure has not been modified, because it is conserved in all probability in every GPCR. On the other hand we have no information about the side chain conformations, so we were allowed to modify the important ones to form the antagonist binding cavity. For the flexible docking 16 rotatable bonds in the side chains of the receptor model were defined: Asp 107, Tyr 108, Trp 158, Phe 199, Trp 428, Tyr 431, Phe 432 and Phe 435. In the ligands all rotatable bonds were allowed free to move. After the docking process every binary complex structures were refined with the Powell algorithm [28] using the MMFF94 force field [30] and charges, with a non-bonded cutoff of 9 Å and distance dependent dielectric constant ($\epsilon = 4r$). During the geometry optimization the backbone atoms were treated as frozen aggregates.

Mepyramine was chosen from the first-generation antihistamines for the first ligand to be docked, which binds to HHR1 with high affinity [9]. The docked mepyramine has created a strong ionic interaction with Asp 107, and its two aryl groups were found in the lipophilic cavity, formed by Tyr 108, Trp 158, Phe 184, Phe 190, Phe 199, Phe 424, Trp 428, Tyr 431, Phe 432 and Phe 435 (Fig. 8).

For the second ligand, we chose desloratadine—a potent and selective ligand with a dibenzoazepine structure [9]. Desloratadine is a rigid molecule without any rotatable bond. The docked desloratadine's protonated amine group is in an ionic interaction with the carboxylate group of Asp 107, and the condensed ring system was fitted well into the lipophilic binding cavity (Fig. 9).

A related molecule, loratadine, was docked into the HHR1 model, as well. The structural difference between desloratadine and loratadine is negligible, although desloratadine is

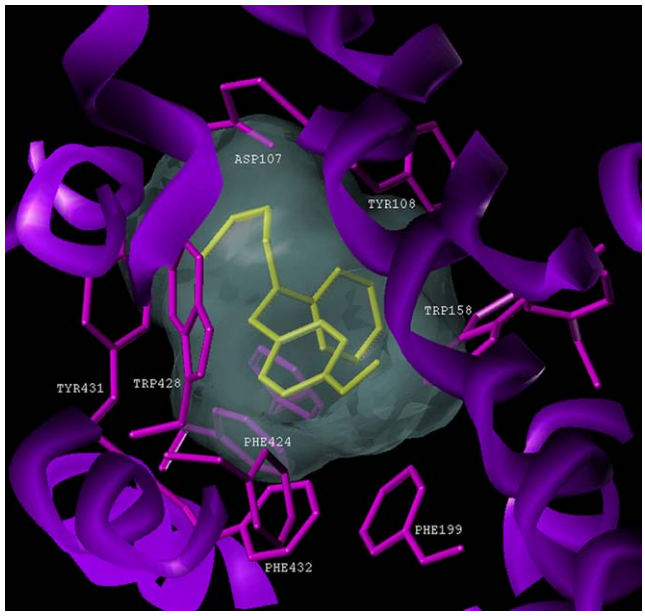


Fig. 8. Binding mode of mepyramine within the active site of HHR1. Residues that are important in forming the active site are coloured violet and labelled. Mepyramine, coloured yellow, is represented in capped stick rendering within its translucent van der Waals surface.

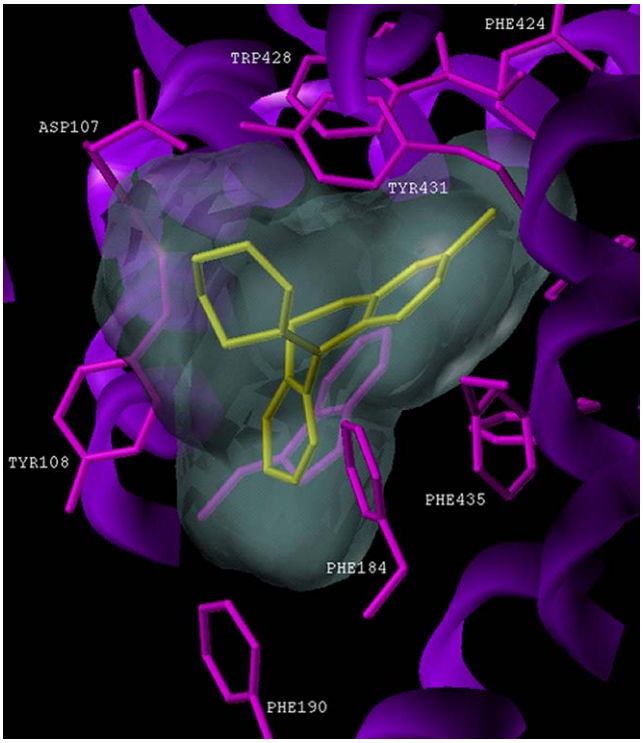


Fig. 9. Binding mode of desloratadine within the active site of HHR1. Residues that are important in forming the active site are coloured violet and labelled. Desloratadine, coloured yellow, is represented in capped stick rendering within its translucent van der Waals surface.

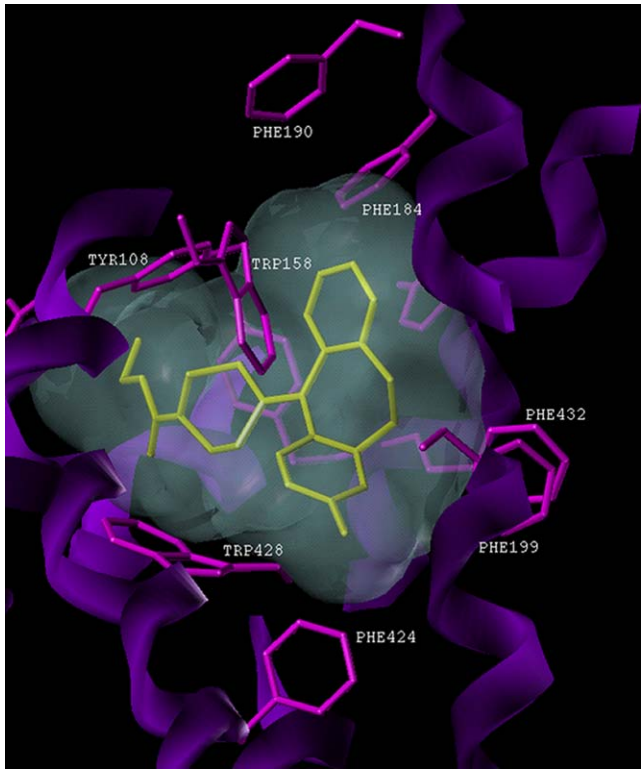


Fig. 10. Binding mode of loratadine within the active site of HHR1. Residues that are important in forming the active site are coloured violet and labelled. Loratadine, coloured yellow, is represented in capped stick rendering within its translucent van der Waals surface.

153 times more potent, than loratadine [9]. We presumed, that the reason for this notable affinity difference is that loratadine's amine group cannot interact with Asp 107, since it is not protonated in physiological pH [26]. As a result, loratadine's deprotonated amine group was found far away from the carboxylate of Asp 107, but has created lipophilic interactions with the previously described aromatic residues of the receptor (Fig. 10).

Some H1 antagonist (acrivastine, cetirizine, olopatadine, fexofenadine) contain a carboxylate group, which reduces side effects considerably, because these compounds are unable to cross the BBB. A specific interaction point was supposed to be in HHR1 [6], which can interact with the deprotonated carboxylate group of these zwitterionic molecules. Mutational studies in guinea pig H1 receptor have proved, that Lys 200 (Lys 191 in HHR1) has a major role in the binding of acrivastine and cetirizine [9]. Acrivastine has high affinity for H1 receptor, and was affected by the K200A guinea pig mutation 6–7 times more than cetirizine, therefore we chose acrivastine to dock into our HHR1 model, with regard to the possible formation of a strong second ionic interaction. Here, the side chain of Lys 191 was let also free to rotate in the binding cavity. As a result, two ionic interactions have been formed between Asp 107 and acrivastine's protonated amine group, and between Lys 191 and acrivastine's deprotonated carboxylate group. The two aromatic rings of the molecule were found in the lipophilic cavity of HHR1 (Fig. 11).

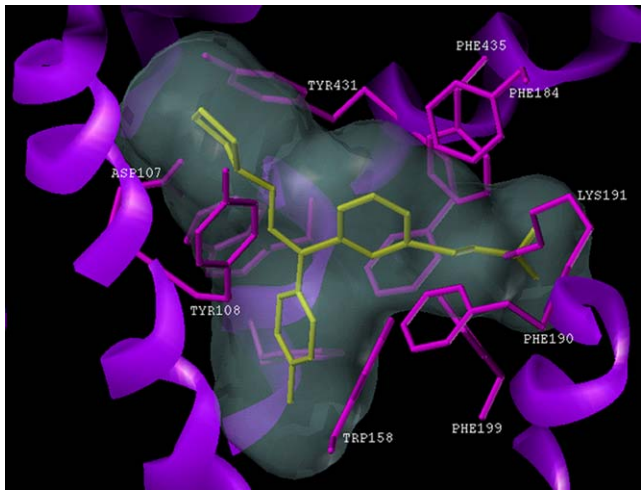


Fig. 11. Binding mode of acrivastine within the active site of HHR1. Residues that are important in forming the active site are coloured violet and labelled. Acrivastine, coloured yellow, is represented in capped stick rendering within its translucent van der Waals surface.

## 4. Discussion

Investigating the distance data of the histamine binding residues (Asp 107, Asn 198, Lys191, Trp 158) led us to a recognition, that TM3 and TM5 are with 1–2 Å too far from each other for an optimal histamine binding. Similar results were obtained in ter Laak's study [13], but they explained it with the incorrectness of their homology model, which used

the non-GPCR bacteriorhodopsin crystal structure as a template. Since we used the high resolution structure of bovine rhodopsin as a template the unacceptable orientation of the histamine binding residues can not simply be the consequence of the low resolution bacteriorhodopsin template. Contrary, we suggest here an alternative explanation for the elongated distance between TM3 and TM5: our receptor model is based on the homology between HHR1 and the bovine rhodopsin receptor's inactive form. Docking an agonist into an inactive receptor state with an aggregated frozen backbone does not make any sense, since agonists' activation mechanism goes with major changes in receptor conformation. The IC3 region and the C-terminal part form the G-protein binding domain of GPCRs. The most probable activation mechanism of HHR1 seems to be the altering of the IC3 region, containing 23 serin and 10 threonin residues as potential sites for phosphorylation. This IC3 part is the continuation of the TM5 region. A TM5 shifting due histamine binding could result a notable change in the IC3—Ser and Thr residues getting in a different position, which makes them accessible for kinase/phosphatase enzymes. We found that Lys 191's hydrogens are in 11–12 Å distance to Asp 107's carboxylate oxygens. This is too long for two favourable H-bonds with histamine's protonated amine group and N($\pi$), since the distance between these two parts of histamine is a bit more, than 5 Å. Optimizing the position of histamine's imidazole ring for two H-bonds with Lys 191 and Asn 198 (with a 3 Å distance) causes the protonated amine group of histamine getting far from Asp 107's carboxylate oxygens, just like the experiences in ter Laak' study [13]. Mutation data show, that Asp 107 and Asn 198 are the most important residues in histamine binding. These amino acids are in a favourable distance from each other to bind histamine's protonated amine group and N($\tau$). These findings show, that Asp 107 and Asn 198 are in a good position for histamine binding, but Lys 191 is not able to reach histamine's N($\pi$) in the inactive form of the HHR1. Mutating Lys 200 (Lys 191 in HHR1) and Asn 207 (Asn 198 in HHR1) in guinea pig H1 receptor can give an explanation for that [31,32]. N207A mutant receptor (N198 in HHR1) has almost no affinity for histamine, therefore we suggest, that Asn 198 and Asp 107 are the most important histamine anchoring residues in HHR1—in absence of them histamine has no affinity for HHR1, which means a total loss of receptor stimulation, as well. In the absence of Lys 191, HHR1 still has an intermediate affinity for histamine, but the receptor stimulation is 50 times lowered—Lys 191 therefore suggested to take part in the HHR1 activation mechanism. On the basis of this observation one can speculate that Asp 107 and Asn 198 are in a good orientation to bind histamine, so in all probability, they will not change their position remarkable during activation. Lys 191 can move in the direction of TM3, with a stable position of Asn 198 that results in a rotation of TM5 around Asn 198. This causes a notable change in the continuation of TM5, which is IC3—the G-protein binding part of HHR1.

Several residues were proved to take part in antagonist binding (Asp 107, Trp 158, Phe 432 and Phe 435), that were found in the internal side of our receptor. On the other hand, Trp 152 faced to the phospholipid bilayer, moreover it was far away from the binding cavity, however mutating this residue results in a total loss of affinity for all H1 ligand. It is clear, that Trp 152 cannot take part in either agonist- or antagonist binding according to our model. The essential role can be explained by the GPCRs' special structure. This Trp 152 residue can be found in almost every GPCR in TM4 in position 11. It takes part in creating an H-bond network with other well conserved polar residues, furthermore it makes a strong lipophilic interaction with the cell membrane [5]. Therefore, the W152A mutant receptor has got a significantly perturbed 3D-structure, which makes a free pass for small ligands to the interior of the cell [6].

As a result of the first docking we got a favourable mepyramine—HHR1 interaction, which satisfied all published mutation data: the carboxylate group of Asp 107 interacts with mepyramine's protonated amine group, and all aromatic amino acids (Tyr 108, Trp 158, Phe 184, Phe 190, Phe 199, Phe 424, Trp 428, Tyr 431, Phe 432, Phe 435) take part in forming a notable lipophilic binding cavity for mepyramine's two aromatic rings. Three of them (Trp 158, Phe 432, Phe 435) have already been proven to be essential or almost indispensable for mepyramine binding [6]. Then again, mepyramine has not formed any interaction with Lys 191, Thr 194 or Asn 198 in keeping with K191A, T194A and N198A mutations, that did not affect the binding affinity of mepyramine [22,33].

Other antihistamines, such as chlorpheniramine, diphenhydramine, tripelennamine, triprolidine, chlorcyclizine and chloropyramine, have got a very similar structure to mepyramine, therefore, they have likely similar binding modes to HHR1, as mepyramine.

A tricyclic H1 antagonist desloratadine was our second choice to dock into the HHR1 model. According to our expectations, desloratadine's amine group was found close enough to Asp 107 to create a strong ionic interaction, and the aromatic rings were fitted in the lipophilic cavity.

The next ligand, loratadine, has not formed any ionic interaction with HHR1, but it was fitted well in the lipophilic cavity. Furthermore, loratadine has not formed any interaction with Thr 194 or Lys 191, which is in agreement with mutation data [32]. Desloratadine is 153 times more potent, than loratadine. On the basis of measured p$K_a$ values [26] of loratadine (p$K_a$ = 4.85) and desloratadine (p$K_a$ = 8.65) we suggest, that the reason of the notable affinity difference is that in physiological pH loratadine's amine group is deprotonated. This difference in p$K_a$ values and consequently in protonation states is because of the electrophilic ethyl–esther group of loratadine, which reduces the basicity of the molecule.

Other tricyclic H1 antagonists (doxepin, ketotifen, epinastine, promethazine and chlorpromazine) are supposed to bind to the same part of HHR1, because of the high similarity between these compounds and desloratadine or loratadine.

The last H1 antagonist, that we docked into HHR1 was acrivastine. As the mutation data have shown [6], Lys 191 has

a major role in the binding of this zwitterionic H1 antagonist. In the acrivastine—HHR1 complex two strong ionic interactions were formed, namely with Asp 107 and Lys 191. In all probability every other zwitterionic ligand's carboxylate group interacts with Lys 191, which is the only positively charged residue in the HHR1 binding cavity.

In conclusion, homology modelling resulted in a human histamine H1 receptor model, which was used to identify the role of several amino acids having an effect on agonist or antagonist binding. We found seven new potential aromatic interaction points in the HHR1 (Tyr 108, Phe 184, Phe 190, Phe 199, Phe 424, Trp 428, Tyr 431), that took part in forming the lipophilic side of the antagonist binding cavity with other residues (Asp 107, Trp 158, Lys 191, Phe 432, Phe 435), proved previously to play a role in antagonist binding. Four known H1 antagonists were docked successfully into our HHR1 model, among others the zwitterionic acrivastine, which created two ionic interactions with Asp 107 and Lys 191. Our docking results are in agreement with experimental site-directed mutagenesis data.

## Acknowledgements

The financial support provided by the Grant OTKA (T 042933) of the Hungarian National Research Fund is gratefully acknowledged.

## References

[1] S.J. Hill, C.R. Ganellin, H. Timmerman, J.C. Schwartz, N.P. Shankley, J.M. Young, W. Schunack, R. Levi, H.L. Haas, Pharmacol. Rev. 49 (1997) 253–278.
[2] T.A. Esbenshade, K.M. Krueger, T.R. Miller, C.H. Kang, L.I. Denny, D.G. Witte, B.B. Yao, G.B. Fox, R. Faghih, Y.L. Bennani, M. Williams, A.A. Hancock, J. Pharmacol. Exp. Ther. 305 (2003) 887–896.
[3] K.L. Morse, J. Behan, T.M. Laz, R.E. West, S.A. Greenfeder, J.C. Anthes, S. Umland, Y. Wan, R.W. Hipkin, W. Gonsiorek, N. Shin, E.L. Gustafson, X. Qiao, S. Wang, J.A. Hedrick, J. Greene, M. Bayne, F.J. Monsma, J. Pharmacol. Exp. Ther. 296 (2001) 1058–1066.
[4] M. O'Reilly, R. Alpert, S. Jenkinson, R.P. Gladue, S. Foo, S. Trim, B. Peter, M. Trevethick, M. Fidock, J. Recept Signal Transduct. Res. 22 (2002) 431–448.
[5] A.L. Lomize, I.D. Pogozheva, H.I. Mosberg, J. Comput. Aided Mol. Des. 13 (1999) 325–353.
[6] K. Wieland, A.M. Laak, M.J. Smit, R. Kuhne, H. Timmerman, R. Leurs, J. Biol. Chem. 274 (1999) 29994–30000.
[7] E.O. Meltzer, Clin. Exp. Allergy 28 (1998) 27–36.
[8] H. Nonaka, S. Otaki, E. Ohshima, M. Kono, H. Kase, K. Ohta, H. Fukui, M. Ichimura, Eur. J. Pharmacol. 345 (1998) 111–117.
[9] J.C. Anthes, H. Gilchrest, C. Richard, S. Eckel, D. Hesk, R.E. West, S.M. Williams, S. Greenfeder, M. Billah, W. Kreutner, R.E. Egan, Eur. J. Pharmacol. 449 (2002) 229–237.
[10] A. Clark, H. Love, Int. J. Cardiol. 33 (1991) 165–167.
[11] R.L. Woosley, Y. Chen, J.P. Freiman, R.A. Gillis, JAMA 269 (1993) 1532–1536.
[12] K. Ohta, H. Hayashi, H. Mizuguchi, H. Kagamiyama, K. Fujimoto, H. Fukui, Biochem. Biophys. Res. Commun. 203 (1994) 1096–1101.
[13] A.M. ter Laak, H. Timmerman, R. Leurs, P.H. Nederkoorn, M.J. Smit, G.M. Donne-Op den Kelder, J. Comput. Aided Mol. Des. 9 (1995) 319–330.
[14] W. Kreutner, J.A. Hey, J. Anthes, A. Barnett, S. Young, S. Tozzi, Arzneimittelforschung 50 (2000) 345–352.
[15] P.J. Mauser, W. Kreutner, R.W. Egan, R.W. Chapman, Eur. J. Pharmacol. 182 (1990) 125–129.
[16] C. Bissantz, P. Bernard, M. Hibert, D. Rognan, Proteins 50 (2003) 5–25.
[17] X.Q. Xie, J.Z. Chen, E.M. Billings, Proteins 53 (2003) 307–319.
[18] T. Klabunde, G. Hessler, G Chembiochem 3 (2002) 928–944.
[19] J.D. Thompson, D.G. Higgins, T.J. Gibson, Nucleic Acids Res. 22 (1994) 4673–4680.
[20] A. Sali, T.L. Blundell, J. Mol. Biol. 234 (1993) 779–815.
[21] K. Palczewski, T. Kumasaka, T. Hori, C.A. Behnke, H. Motoshima, B.A. Fox, I. Le Trong, D.C. Teller, T. Okada, R.E. Stenkamp, M. Yamamoto, M. Miyano, Science 289 (2000) 739–745.
[22] R.A. Laskowski, M.W. MacArthur, D.S. Moss, J.M. Thorton, J. Appl. Crystallogr. 26 (1993) 283–291.
[23] M.J. Sippl, J. Comp. Aided Mol. Des. 7 (1993) 473–501.
[24] G. Vriend, C. Sander, J. Appl. Cryst. 26 (1993) 47–60.
[25] B. Noszal, D.L. Rabenstein, J. Phys. Chem. 95 (1991) 4761–4765.
[26] A.M. ter Laak, R.S. Tsai, G.M. Donné-Op den Kelder, P.A. Carrupi, B. Testa, H. Timmerman, Eur. J. Pharm. Sci. 2 (1994) 373–384.
[27] Pallas, version 3.1; CompuDrug International, Inc., 115 Morgan Drive, Sedona, AZ 86351, USA.
[28] SYBYL, version 6.9; Tripos Inc.: St. Louis, MO.
[29] R. Judson, "Genetic Algorithm and Their Use in Chemistry", in: K.B. Lipkowitz, D.B. Boyd (Eds.), Reviews in Computational Chemistry, 10, VCH Publishers, New York, 1997.
[30] T.A. Halgren, J. Am. Chem. Soc. 112 (1990) 4710–4723.
[31] R. Leurs, M.J. Smit, R. Meeder, A.M. ter Laak, H. Timmerman, Biochem. Biophys. Res. Commun. 214 (1995) 110–117.
[32] R. Leurs, M.J. Smit, C.P. Tensen, A.M. ter Laak, H. Timmerman, Biochem. Biophys. Res. Commun. 201 (1994) 295–301.
[33] M. Gillard, C. van der Perren, N. Moguilevsky, R. Massingham, P. Chatelain, Mol. Pharmacol. 61 (2001) 391–399.